INTERNATIONAL JOURNAL FOR NUMERICAL METHODS IN FLUIDS
Int. J. Numer. Meth. Fluids 2004; **44**:1279–1298 (DOI: 10.1002/fld.618)

Biomagnetic fluid flow in a 3D rectangular duct

E. E. Tzirtzilakis[1], V. D. Sakalis[2], N. G. Kafoussias[1,*,†] and P. M. Hatzikonstantinou[2]

[1]*Department of Mathematics, University of Patras, Section of Applied Analysis, Patras 26500, Greece*
[2]*Department of Engineering Science, University of Patras, Patras 26500, Greece*

SUMMARY

The laminar, incompressible, three-dimensional, fully developed viscous flow of a non-conducting biomagnetic fluid in a impermeable rectangular duct is numerically studied in the presence of an applied magnetic field. It is assumed that the magnetic field strength is sufficiently strong to saturate the biofluid and the magnetization is given as a function of the magnetic field intensity. The system of the partial differential equations, resulting after the introduction of appropriate non-dimensional variables, is solved applying an efficient numerical technique based on a pressure-linked pseudotransient method on a common grid. Results concerning the existence and the uniqueness of the solution, are also given. The obtained results, for different values for the parameters entering into the problem under consideration, show that the flow is appreciably influenced by the presence of the magnetic field. Copyright © 2004 John Wiley & Sons, Ltd.

KEY WORDS: biomagnetic fluid; numerical; existence and uniqueness of solution of pde; pressure linked

1. INTRODUCTION

The influence of the magnetic field on the flow of biofluids is extensively investigated because of numerous applications in medicine [1–3].

The most famous biofluid, the flow of which is influenced by the presence of a magnetic field, is blood. Blood, specifically, holds the properties of a magnetic fluid because of the existence of a form of iron oxides in the haemoglobin molecule, which appears at very high concentrations at the mature red blood cells. It was found that the erythrocytes orient with their disk plane parallel to the magnetic field [4–6] and also that the blood possesses the property of diamagnetic material when oxygenated and of paramagnetic material when deoxygenated [7].

*Correspondence to: N. G. Kafoussias, Department of Mathematics, University of Patras, Patras 26500, Greece.
†E-mail: nikaf@math.upatras.gr

Contract/grant sponsor: Karatheodoris program of the Research Committee University of Patras; contract/grant number: 2439

Received 14 August 2002
Accepted 14 April 2003

In order to investigate the flow of a biomagnetic fluid, the biomagnetic fluid dynamics (BFD) has been developed [8]. The mathematical formulation of BFD is analogous to the one of ferrohydrodynamics (FHD), which deals with no electric current, and considers that the flow is affected by the magnetization of the fluid in the magnetic field. Thus, the resulting equations of BFD are taking into account the magnetization of the fluid, as opposed to the formulation in magnetohydrodynamics (MHD), which deals with conducting fluids and the corresponding mathematical model ignores the effect of polarization and magnetization.

So, in the present study, we investigate the laminar, incompressible, three-dimensional, fully developed, viscous flow of a non-conducting biomagnetic fluid in a impermeable rectangular duct under the influence of an applied magnetic field, using a simplified BFD model. The magnetization M is considered as a function of the magnetic field intensity H. For the numerical solution of the problem we develop a simple and efficient technique based on a pseudotransient pressure-linked equation model on a co-located grid. Special care is taken in order to avoid oscillatory solutions and divergence. We additionally demonstrate results regarding the existence of solution we compute numerically.

The results concerning the velocity field and skin friction, show that the flow is appreciably influenced by the magnetic field. The presence of the magnetic field leads to the appearance of secondary flow whereas the axial velocity is considerably reduced.

2. MATHEMATICAL FORMULATION

We consider the laminar, incompressible, three-dimensional viscous flow, of an electrically non-conducting biomagnetic fluid in a impermeable rectangular duct of square cross-section of side h. The flow is subjected to the action of an applied magnetic field of sufficient strength to saturate the biomagnetic fluid. The magnetic field is generated by an electric current going through a thin wire placed parallel to the axis of symmetry of the bottom plane of the duct, at distance c below it. As it is shown in Figure 1(a), the flow is studied at a representative cross-section ABCD with the origin of the co-ordinate system placed at the point A, while in Figure 1(b) the contours of the intensity of the magnetic field $\mathbf{H}$ are shown.

The mathematical model for the BFD is based on the modified Stokes principles and on the assumption that besides the three thermodynamic variables, e.g. pressure P, density ρ and temperature T, the biomagnetic fluid behaviour depends on the magnetization M [8], which is a measure of the effect of the magnetic field on the magnetic fluid.

The linear equation relating the magnetization $\bar{M}$ with the strength intensity of the magnetic field $\bar{H}$ and the temperature $\bar{T}$, is given by $\bar{M} = \bar{K}\bar{H}(\bar{T}_c - \bar{T})$, where $\bar{T}_c$ is the Curie temperature and $\bar{T}$ is the fluid temperature [9]. However, for negligible temperature differences we can consider that the magnetization $\bar{M}$ is given only as a function of the magnetic field intensity $\bar{H}$, so that $\bar{M} = \bar{K}\bar{H}$, where $\bar{K}$ is a constant and $\bar{H}_0$ is the magnetic field strength at the point $(h/2, 0)$.

Thus, considering that the temperature changes are insignificant and a magnetic field sufficiently strong to saturate the biofluid we conclude that the governing equations of the fluid flow are similar to those derived in ferrohydrodynamics [10, 11]. Hence, at the fully developed flow the dimensional velocity components of $\mathbf{V} = (\bar{u}, \bar{v}, \bar{w})$ and the pressure $\bar{P}$ are governed by the mass conservation and the fluid momentum equations at the $\bar{x}$, $\bar{y}$ and $\bar{z}$ directions,

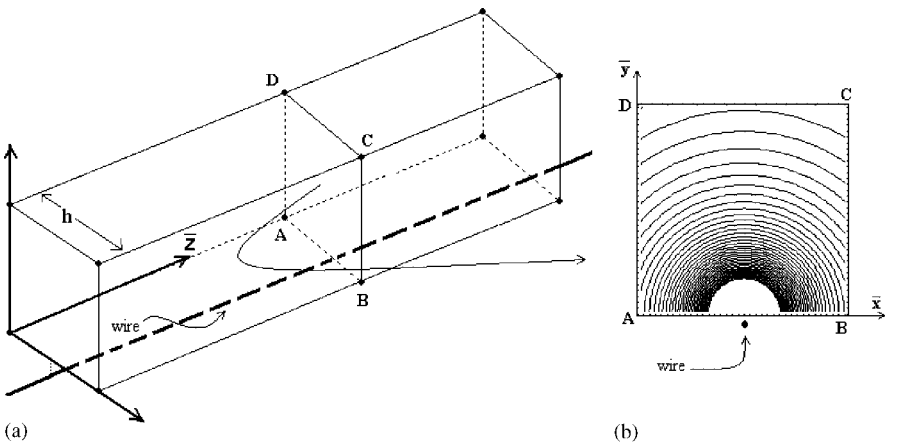

Figure 1. The flow configuration. The contours of the magnetic field strength $\bar{H}$ are shown in the ABCD plane of the cross-section.

which are given, respectively, by

$$\frac{\partial \bar{u}}{\partial \bar{x}} + \frac{\partial \bar{v}}{\partial \bar{y}} = 0 \tag{1}$$

$$\frac{\partial \bar{u}}{\partial \bar{t}} + \bar{u}\frac{\partial \bar{u}}{\partial \bar{x}} + \bar{v}\frac{\partial \bar{u}}{\partial \bar{y}} = -\frac{1}{\bar{\rho}}\frac{\partial \bar{P}}{\partial \bar{x}} + \bar{\nu}\left\{\frac{\partial^2 \bar{u}}{\partial \bar{x}^2} + \frac{\partial^2 \bar{u}}{\partial \bar{y}^2}\right\} + \frac{\bar{\mu}_0 \bar{M}}{\bar{\rho}}\frac{\partial \bar{H}}{\partial \bar{x}} \tag{2}$$

$$\frac{\partial \bar{v}}{\partial \bar{t}} + \bar{u}\frac{\partial \bar{v}}{\partial \bar{x}} + \bar{v}\frac{\partial \bar{v}}{\partial \bar{y}} = -\frac{1}{\bar{\rho}}\frac{\partial \bar{P}}{\partial \bar{y}} + \bar{\nu}\left\{\frac{\partial^2 \bar{v}}{\partial \bar{x}^2} + \frac{\partial^2 \bar{v}}{\partial \bar{y}^2}\right\} + \frac{\bar{\mu}_0 \bar{M}}{\bar{\rho}}\frac{\partial \bar{H}}{\partial \bar{y}} \tag{3}$$

$$\frac{\partial \bar{w}}{\partial \bar{t}} + \bar{u}\frac{\partial \bar{w}}{\partial \bar{x}} + \bar{v}\frac{\partial \bar{w}}{\partial \bar{y}} = -\frac{1}{\bar{\rho}}\frac{\partial \bar{P}}{\partial \bar{z}} + \bar{\nu}\left\{\frac{\partial^2 \bar{w}}{\partial \bar{x}^2} + \frac{\partial^2 \bar{w}}{\partial \bar{y}^2}\right\} \tag{4}$$

The boundary conditions of the problem are

$$\bar{y} = 0 \text{ or } \bar{y} = h \quad \text{and} \quad 0 \leqslant \bar{x} \leqslant h\text{:}\ \ \bar{u} = \bar{v} = \bar{w} = 0 \tag{5}$$

$$\bar{x} = 0 \text{ or } \bar{x} = h \quad \text{and} \quad 0 \leqslant \bar{y} \leqslant h\text{:}\ \ \bar{u} = \bar{v} = \bar{w} = 0 \tag{6}$$

In the above-dimensional equations, $\bar{\rho}$ is the biomagnetic fluid density, $\bar{\nu}$ is the kinematic viscosity and $\bar{\mu}_0$ the magnetic permeability.

The terms $\bar{\mu}_0\bar{M}(\partial\bar{H}/\partial\bar{x})/\bar{\rho}$ and $\bar{\mu}_0\bar{M}(\partial\bar{H}/\partial\bar{y})/\bar{\rho}$ in (2) and (3), represent the components of the magnetic force per unit mass along the $\bar{x}$ and $\bar{y}$ axes, respectively. However, the magnetic force component along the z-direction vanishes because $\partial\bar{H}/\partial\bar{z} = 0$.

The components of the magnetic field intensity $\bar{H}_x$ and $\bar{H}_y$ along the $\bar{x}$ and $\bar{y}$ co-ordinates, $(\mathbf{H}=(\bar{H}_x,\bar{H}_y))$ are given, respectively, by

$$\bar{H}_x=\frac{\gamma}{2\pi}\frac{\bar{x}-a}{(\bar{x}-a)^2+(\bar{y}-b)^2},\quad \bar{H}_y=-\frac{\gamma}{2\pi}\frac{\bar{y}-b}{(\bar{x}-a)^2+(\bar{y}-b)^2}$$

for the problem under consideration $\alpha=h/2$ and $b=-c$ (see Figure 1). The magnitude $\bar{H}$, of the magnetic field intensity, is given by

$$\bar{H}(\bar{x},\bar{y})=[\bar{H}_x^2+\bar{H}_y^2]^{1/2}=\frac{\gamma}{2\pi}\frac{1}{(\bar{x}-a)^2+(\bar{y}-b)^2} \tag{7}$$

where γ is the magnetic field strength at the point $(\bar{x}=a,\bar{y}=b)$.

3. TRANSFORMATION OF EQUATIONS

Introducing the non-dimensional variables

$$\begin{aligned} &x=\frac{\bar{x}}{h},\quad y=\frac{\bar{y}}{h},\quad z=\frac{\bar{z}}{h},\quad u=\frac{\bar{u}h}{\bar{\nu}},\quad v=\frac{\bar{v}h}{\bar{\nu}},\quad w=\frac{\bar{w}h}{\bar{\nu}}\\ &P=\frac{\bar{P}}{\bar{\rho}\bar{\nu}^2/h^2},\quad H=\frac{\bar{H}}{\bar{H}_0},\quad t=\frac{\bar{t}\bar{\mu}}{\bar{\rho}h^2}\end{aligned} \tag{8}$$

and splitting the pressure as in Reference [12] under the assumption of the fully developed flow we have

$$P(x,y,z)=P_1(z)+p(x,y)$$

and

$$\frac{\partial P}{\partial z}=\frac{\partial P_1}{\partial z}\equiv P_z=\text{constant}$$

$$\frac{\partial P}{\partial x}=\frac{\partial p}{\partial x}\equiv P_x\quad\text{and}\quad\frac{\partial P}{\partial y}=\frac{\partial p}{\partial y}\equiv P_y$$

Substituting the above-mentioned relations to (1)–(6) we obtain the equations

$$\frac{\partial u}{\partial x}+\frac{\partial v}{\partial y}=0 \tag{9}$$

$$\frac{\partial u}{\partial t}+u\frac{\partial u}{\partial x}+v\frac{\partial u}{\partial y}=-\frac{\partial p}{\partial x}+\frac{\partial^2 u}{\partial x^2}+\frac{\partial^2 u}{\partial y^2}+\mathrm{Mn}\,H\frac{\partial H}{\partial x} \tag{10}$$

$$\frac{\partial v}{\partial t}+u\frac{\partial v}{\partial x}+v\frac{\partial v}{\partial y}=-\frac{\partial p}{\partial y}+\frac{\partial^2 v}{\partial x^2}+\frac{\partial^2 v}{\partial y^2}+\mathrm{Mn}\,H\frac{\partial H}{\partial y} \tag{11}$$

$$\frac{\partial w}{\partial t}+u\frac{\partial w}{\partial x}+v\frac{\partial w}{\partial y}=-P_z+\frac{\partial^2 w}{\partial x^2}+\frac{\partial^2 w}{\partial y^2} \tag{12}$$

under the boundary conditions

$$y=0 \text{ or } y=1 \quad \text{and} \quad 0\leqslant x\leqslant 1:\ u=v=w=0 \tag{13}$$

$$x=0 \text{ or } x=1 \quad \text{and} \quad 0\leqslant y\leqslant 1:\ u=v=w=0 \tag{14}$$

The parameter $\mathrm{Mn}=h^2\bar{\mu}_0\bar{K}\bar{H}_0^2/(\bar{\nu}^2\bar{\rho})$ is the dimensionless magnetic number. The system of equations (9)–(12), subjected to the boundary conditions (13)–(14), is a one parameter, coupled non-linear system of partial differential equations describing the biomagnetic fully developed fluid flow in a rectangular duct when the magnetization is given as a function of the magnetic field intensity H.

4. NUMERICAL SOLUTION TECHNIQUE

For the study of the steady state of the flow we use a pseudotransient method where the time $\bar{t}$ plays the role of an iteration parameter until the steady state is reached. So, we solve the system of equations (9)–(12), subjected to the boundary conditions (13)–(14), applying a numerical technique based on the pseudotransient pressure-linked equation method (PLEM) briefly mentioned in Reference [12].

It is worth mentioning here that it is unpractical to use the very well-known vorticity-stream function formulation because the cross-differentiation will eliminate not only the pressure but the terms due to magnetic field as well. In addition, the problem under consideration is three-dimensional and consequently, implementation of vorticity-stream function formulation will not considerably simplify the governing equations.

Thus, we use the PLEM scheme using a collocated orthogonal grid, for avoiding the complexity of the discretized differential equations using a staggered grid. In a collocation grid all the variables are determined at the same grid nodes whereas, in a staggered grid each variable is determined at different grid points [12, 13].

The PLEM method allow the following algorithm to be generated from the system of equations (9)–(12).

Let (u^*, v^*, w^*) be an approximate solution of equations (9)–(12) computed numerically for a given value of the axial pressure gradient component P_z and an approximate value of the pressure p^n. The variables u^* and v^* will not satisfy the continuity equation. However, the correction of the velocity components introduces the pressure correction p'. Hence, the required variables are written as

$$u=u^*+u', \quad v=v^*+v', \quad p=p^n+p' \tag{15}$$

Illustrating the determination of the velocity corrections we consider Equation (10) which in terms of the estimated variables u^*, v^* and p^n takes the form

$$\frac{\partial u^*}{\partial t}+u^*\frac{\partial u^*}{\partial x}+v^*\frac{\partial u^*}{\partial y}=-\frac{\partial p^n}{\partial x}+\frac{\partial^2 u^*}{\partial x^2}+\frac{\partial^2 u^*}{\partial y^2}+\mathrm{Mn}\,H\frac{\partial H}{\partial x} \tag{16}$$

Subtracting (16) from (10) and using relations (15), we obtain the following linearized equation for the correction u':

$$\frac{\partial u'}{\partial t} + u^* \frac{\partial u'}{\partial x} + v^* \frac{\partial u'}{\partial y} = -\frac{\partial p'}{\partial x} + \frac{\partial^2 u'}{\partial x^2} + \frac{\partial^2 u'}{\partial y^2} \tag{17}$$

The terms $(\mathbf{V}^* \cdot \nabla)u'$ and $\nabla^2 u'$ usually are neglected in various numerical methods (including the initial SIMPLE algorithm [12, 13]) because their consideration increases substantially the complexity without effecting the accuracy of the method. The small magnitude of the terms $(\mathbf{V}^* \cdot \nabla)u'$ and $\nabla^2 u'$ has been also proved by the numerical calculation of the convection and diffusion terms in Equation (17).

So, omitting the small terms $(\mathbf{V}^* \cdot \nabla)u'$ and $\nabla^2 u'$, from (17), we obtain the equation

$$\frac{\partial u'}{\partial t} = -\frac{\partial p'}{\partial x}$$

Hereafter discretizing the time derivative applying the forward difference $\partial u'/\partial t = (u'^{n+1} - u'^{n})/\Delta t$ and considering that $u' = 0$ at the time step (n) we conclude that the time step $(n+1)$ the correction u' will be given by

$$u'^{n+1} = -\Delta t \frac{\partial p'}{\partial x} \tag{18}$$

Similarly from (11) for the correction v', we obtain

$$v'^{n+1} = -\Delta t \frac{\partial p'}{\partial y} \tag{19}$$

Note that for every time step, the correction of the axial velocity is $w' = 0$, due to the assumption that P_z is a known constant quantity.

At each time step the substitution of (15) into the continuity equation (9), and taking into account (18) and (19), leads to the Poisson equation, for the pressure correction, of the form

$$\frac{\partial^2 p'}{\partial x^2} + \frac{\partial^2 p'}{\partial y^2} = \frac{1}{\Delta t}\left(\frac{\partial u^*}{\partial x} + \frac{\partial v^*}{\partial y}\right) \tag{20}$$

The boundary conditions of the velocities u^*, v^* and w^* at the wall are zero. The boundary conditions for the pressure correction p' are obtained from the values of (18) and (19) where $u' = v' = 0$ at the wall. Hence, the boundary conditions are given by

$$y = 0 \text{ or } y = 1 \quad \text{and} \quad 0 \leqslant x \leqslant 1\text{: } u^* = v^* = w^* = P'_y = 0 \tag{21}$$

$$x = 0 \text{ or } x = 1 \quad \text{and} \quad 0 \leqslant y \leqslant 1\text{: } u^* = v^* = w^* = P'_x = 0 \tag{22}$$

Applying the PLEM method iteratively, by marching in time, it is necessary to give initial guesses $(t = 0)$ at all the grid points of the computational domain. For the pressure gradient $P_z = \text{const}$, we can give any arbitrary negative value. It is noted that in the stagnant situation of the fluid the transverse pressure gradient forces are balanced by the forces due to the affect of the magnetic field [11]. Thus, we start the iteration procedure at the $n = 0$ time level, using, as initial guesses, zero velocities and for the transverse pressure gradients $P_x = \text{Mn}\, H\ (\partial H/\partial x) +$

10^{-12} and $P_y = \mathrm{Mn}\, H\ (\partial H/\partial y) + 10^{-12}$ indicating that the fluid starts moving in the transverse plane.

The values of u^* and v^* for the next iteration, are calculating by the use of the ADI method [12] from Equation (16) for u^*, and the analogous to (16) equation for v^*. Hereafter, replacing the values u^* and v^* into (20) and solving the equation with the SOR method, the pressure correction p' is calculated.

Considering now that p' is known, the corrections u' and v' are also calculated from (18) and (19), respectively. Thus, at each time level $n+1$ the required velocities and the pressure, are now determined by the relations

$$u^{n+1} = u^* + u', \quad v^{n+1} = v^* + v', \quad w^{n+1} = w^*, \quad p^{n+1} = p^n + p' \tag{23}$$

We compare now the new estimations at the time level $n+1$ with the previous ones at the time level n, seeking to differ less than a prescribed quantity ε. If the convergence criterion does not hold, we set the new estimations as the old ones and repeat the iteration procedure till we reach, to high accuracy, the steady state.

Once the solution is found, we calculate the corresponding Reynolds number Re, to the given value of P_z, as well as other quantities of interest in a way described in later session.

It is worth mentioning here, that the use of a common orthogonal grid, does produces oscillatory solutions. However, these oscillations are decreased considerably using one-sided finite differences for the implementation of the pressure gradient boundary conditions (21) and (22), for the solution of (20). For the convergence of the whole scheme also, it is essential to set a limit for the number of iterations of the SOR method solving (20). During the first iterations we observed that Equation (20) could not be solved up to the accuracy ε. So, it is of critical importance to set a maximum number of iterations together with the desired accuracy criterion for the solution of (20).

The criterion of convergence ε was chosen to be 10^{-4} for the maximum absolute difference at all the grid points of the computational domain, between the new estimation of an unknown function f, (f_{new}) at the time level $n+1$ and the old one, f_{old}, at the n time level, i.e. $\max_{i,j} |f_{\mathrm{new}} - f_{\mathrm{old}}| < 10^{-4}$.

5. RESULTS

The main advantage of the numerical technique we described is that it is applicable to a common grid. However, it seems that slightly oscillations still occur and the numerical results are not totally independent on the grid density. We observed that oscillations are increasing not only for relatively sparse grids (40×40 or 50×50), but also for relatively dense ones (90×90 or 100×100).

Let $(\hat{u}, \hat{v}, \hat{w}, \hat{p})$ the evaluated solution at all the grid points (i, j) of the computational domain and Equation (10):

$$\frac{\partial u}{\partial t} + u\frac{\partial u}{\partial x} + v\frac{\partial u}{\partial y} + P_x - \frac{\partial^2 u}{\partial x^2} - \frac{\partial^2 u}{\partial y^2} - \mathrm{Mn}\, H\frac{\partial H}{\partial x} = 0$$

Table I. Residuals of the continuity and the u, v and w momentum equations, respectively, for various grids.

Grid	ResCont	Resu	Resv	Resw	Mn
60×60	0.391×10^{-5}	0.494×10^{-3}	0.400×10^{-3}	0.371	0.0
60×60	0.194×10^{-1}	0.803×10^{-1}	0.856×10^{-1}	0.369	0.1×10^{7}
60×60	0.349×10^{-1}	0.706×10^{-1}	0.745×10^{-1}	0.375	0.2×10^{7}
60×60	0.455×10^{-1}	0.910×10^{-1}	0.949×10^{-1}	0.392	0.3×10^{7}
60×60	0.523×10^{-1}	0.108	0.1118	0.371	0.4×10^{7}
60×60	0.420×10^{-1}	0.429×10^{-1}	0.434×10^{-1}	0.818×10^{-1}	0.5×10^{7}
75×75	0.288×10^{-5}	0.266×10^{-3}	0.248×10^{-3}	0.575	0.0
75×75	0.330×10^{-5}	0.283×10^{-3}	0.266×10^{-3}	0.576	0.1×10^{7}
75×75	0.421×10^{-5}	0.380×10^{-3}	0.357×10^{-3}	0.577	0.2×10^{7}
75×75	0.725×10^{-5}	0.594×10^{-3}	0.617×10^{-3}	0.578	0.3×10^{7}
75×75	0.116×10^{-4}	0.660×10^{-3}	0.666×10^{-3}	0.586	0.4×10^{7}
75×75	0.325×10^{-4}	0.755×10^{-3}	0.717×10^{-3}	0.619	0.5×10^{7}
100×100	0.372×10^{-5}	0.770×10^{-3}	0.726×10^{-3}	0.103×10	0.0
100×100	0.435×10^{-2}	0.284×10^{-2}	0.266×10^{-2}	0.104×10	0.1×10^{7}
100×100	0.827×10^{-2}	0.410×10^{-2}	0.399×10^{-2}	0.104×10	0.2×10^{7}
100×100	0.117×10^{-1}	0.564×10^{-3}	0.743×10^{-3}	0.104×10	0.3×10^{7}
100×100	0.148×10^{-1}	0.973×10^{-2}	0.947×10^{-2}	0.104×10	0.4×10^{7}
100×100	0.176×10^{-1}	0.834×10^{-3}	0.121×10^{-2}	0.104×10	0.5×10^{7}

If the evaluated solution is substituted in the above equation it will not give exactly zero at each (i,j) point but

$$\frac{\partial \hat{u}}{\partial t} + \hat{u}\frac{\partial \hat{u}}{\partial x} + \hat{v}\frac{\partial \hat{u}}{\partial y} + \hat{P}_x - \frac{\partial^2 \hat{u}}{\partial x^2} - \frac{\partial^2 \hat{u}}{\partial y^2} - \mathrm{Mn}\, H \frac{\partial H}{\partial x} = R_{i,j} \tag{24}$$

The time and spatial derivatives are calculated by backward and central differences, respectively, at the (i,j) point.

The residual for this equation, Resu, is defined as

$$\mathrm{Res\,u} = \frac{1}{MN}\sum_{i=1}^{M}\sum_{j=1}^{N}|R_{i,j}|$$

where, M and N is the number of grid points at the x and y directions, respectively. In an analogous way, we define the residuals for Equations (9), (11), (12) as ResCont, Resv and Resw, respectively. The obtained results, shown in Table I, indicate that the best choice for the grid is 75×75.

For the category of the numerical methods under consideration (pressure linked) the accuracy is not computed easily and can be at most $O(\Delta x^2) + O(\Delta y^2)$ [12, 13]. For the case of the 75×75 grid the discretization with central differences of (24) is of the order of 10^{-4}.

Keeping in mind that the u and v velocity components are varying from 10–100 the residuals calculated for the continuity, x and y momentum equations are of the same order of discretization of the exact equations and thus, very satisfactory. Moreover, the w velocity component

takes maximum values 580–420 as the magnetic field strength varies from $0–5 \times 10^6$ and the corresponding residual of 0.57, as defined above, is satisfactory enough, resulting to 1–2% error.

Clearly, the oscillations in the case of the sparse grids are increasing due to the truncation errors of the finite-difference approximations of the related equations, whereas, for the dense ones is due to the round of errors. Thus, the spatial step at the x and y directions is taken as $\Delta x = \Delta y = \frac{1}{75}$. The minimization of errors, based on stability considerations, is achieved for time step $\Delta t \leqslant ((\Delta x^2 + \Delta y^2)/2)/6$ [14], so that we choose $\Delta t = ((\Delta x^2 + \Delta y^2)/2)/6$. Calculations where made also for $\Delta t = ((\Delta x^2 + \Delta y^2)/2)/60$ and no differences where found.

The use of a collocated grid in pressure-linked equation methods, may result to the appearance of oscillatory solutions [12, 13]. In our method, these oscillations are decreased considerably by using one-sided third-order inward finite differences for the implementation of the pressure gradient boundary conditions (21) and (22), for the solution of (20). The use of these boundary conditions together with the choice of the best grid, presented above, eliminates the appearing oscillations in the solution as it can be seen from the obtained results.

The mean velocity $\bar{w}_\mathrm{m}$ passing through the cross-section ABCD (see Figure 1) is given by

$$\bar{w}_\mathrm{m} = \frac{1}{h^2} \int_0^h \int_0^h \bar{w} \, \mathrm{d}\bar{x} \, \mathrm{d}\bar{y} \tag{25}$$

while, the dimensionless mean velocity w_m, using (8), is written

$$w_\mathrm{m} = \frac{\bar{w}_\mathrm{m} h}{\nu} = \int_0^1 \int_0^1 w \, \mathrm{d}x \, \mathrm{d}y \tag{26}$$

Thus, the Reynolds number defined, by $Re = \bar{w}_\mathrm{m} h / \bar{\nu}$, can be written as

$$Re = \int_0^1 \int_0^1 w \, \mathrm{d}x \, \mathrm{d}y \tag{27}$$

and is calculated after the solution of dynamic equations.

It is found that for magnetic field of 8 T the blood ($\bar{\rho} = 1050 \, \mathrm{kg/m^3}$, $\bar{\nu} = 3.1 \times 10^{-6} \, \mathrm{m^2/s}$) [15], has reached saturation magnetization of $M_\mathrm{s} = 60 \, \mathrm{A/m}$ [8]. From the definition of the magnetic number we have

$$\mathrm{Mn} = \frac{h^2 \bar{\mu}_0 \bar{K} \bar{H}_0^2}{\bar{\nu}^2 \bar{\rho}} = \frac{h^2 \bar{B}_0 \bar{M}_0}{\bar{\nu}^2 \bar{\rho}}$$

where $\bar{B}_0 = \bar{\mu}_0 \bar{H}_0$ and $\bar{M}_0 = \bar{K} \bar{H}_0$ is the magnetic field induction and the magnetization at the point (0.5,0), respectively. For $\bar{B}_0 = 8 \, \mathrm{T}$ we assume that the magnetic fluid is saturated ($M_0 = M_\mathrm{s}$) and for $h = 0.01 \, \mathrm{m}$ it is obtained that $\mathrm{Mn} \approx 5 \times 10^6$.

In Figure 2, the axial velocity w is presented graphically for values of the magnetic number $\mathrm{Mn} = 1 \times 10^6 – 5 \times 10^6$. As Mn increases the flow is retarded near the area where the magnetic field is applied.

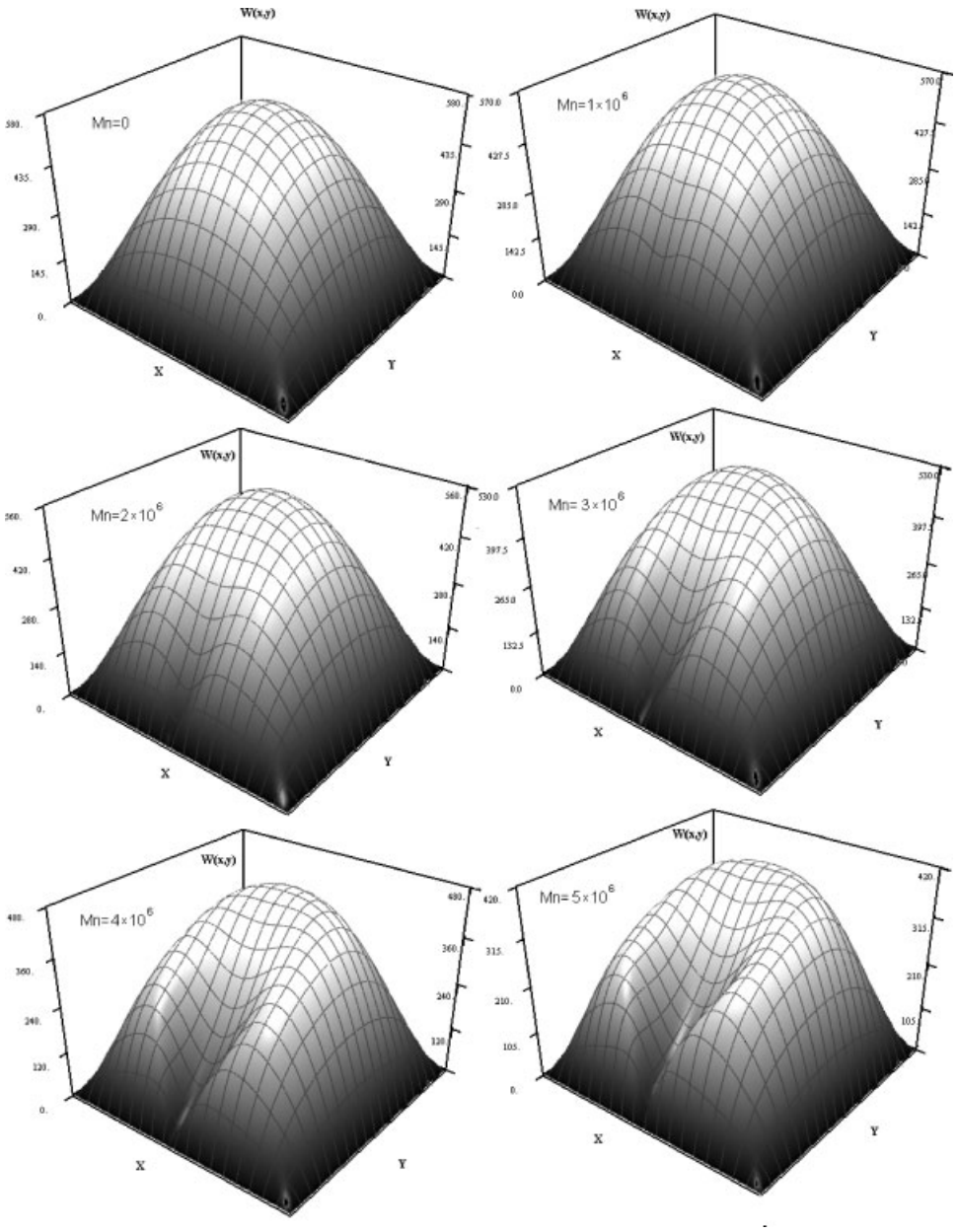

Figure 2. Axial dimensionless velocity w for different values of the magnetic number Mn.

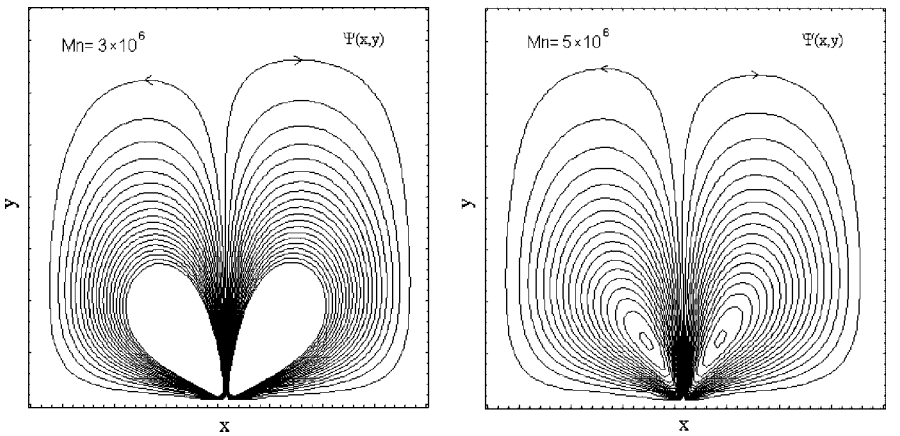

Figure 3. Contours of the stream function $\Psi(x, y)$ for different values of the magnetic number Mn.

The contours of stream function Ψ, defined by the relations

$$u = \frac{\partial \Psi}{\partial y}, \quad v = -\frac{\partial \Psi}{\partial x}$$

are shown in Figure 3, for magnetic number 3×10^6 and 5×10^6, respectively. The stream function is calculated from the vorticity equation

$$\frac{\partial^2 \Psi}{\partial x^2} + \frac{\partial^2 \Psi}{\partial y^2} = -\left(\frac{\partial v}{\partial x} - \frac{\partial u}{\partial y}\right)$$

with boundary conditions $\Psi = 0$ at the wall. It is observed that the magnetic field generates two vortices transferring fluid from both sides of the vertical axe-y at $x = 0.5$ toward the vertical walls of the duct. This secondary flow strengthens with the increase of the applied magnetic field.

An important flow characteristic is the dimensionless skin friction coefficient f of the flow, given by the expression

$$f = \frac{-(\partial \bar{P}/\partial \bar{z})h}{\bar{\rho}\bar{w}_{\mathrm{m}}^2}$$

Using relations (8) and (25)–(27) we obtain the following non-dimensional product:

$$f\,Re = \frac{-P_z}{Re} \tag{28}$$

In order to investigate the influence of the magnetic field in the blood flow we define, for different values of the magnetic number Mn, the number $f\,Re^* = 100((f\,Re - f\,Re_0)/f\,Re_0)$, where $f\,Re_0$ is the $f\,Re$ number for $\mathrm{Mn} = 0$. Consequently, $f\,Re^*$ represents the percentage change of $f\,Re$ due to the presence of the magnetic field. In Table II the obtained Re number, the $f\,Re$ as well as the $f\,Re^*$ numbers are shown for various values of the magnetic number Mn and for axial pressure gradient $P_z = -8000$. It is observed that as Mn increases,

Table II. Variation of Re, $f\,Re$ and $f\,Re^*$ with Mn.

Re	$f\,Re$	$f\,Re^*$	Mn
265.78	15.049	0.000	0.0×10^6
264.20	15.139	0.599	1.0×10^6
258.24	15.489	2.919	2.0×10^6
246.26	16.242	7.925	3.0×10^6
228.03	17.541	16.553	4.0×10^6
207.33	19.292	28.192	5.0×10^6

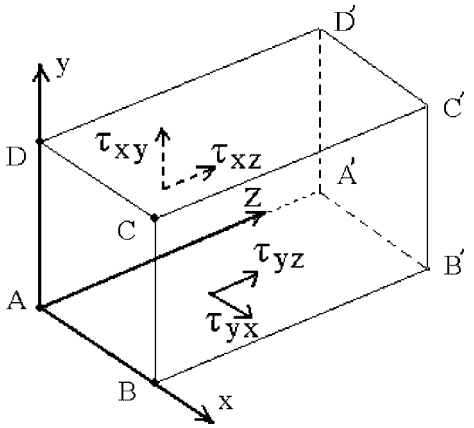

Figure 4. Shear stresses acting on $ABB'A'$ plane (lower wall) and $AA'D'D$ plane (left wall).

the Reynolds number Re decreases whereas the values of $f\,Re^*$ are increased. It is worth mentioning that for an increment in the values of Mn from 0 to 5.0×10^6 the corresponding increment of $f\,Re$ is 28.19%.

As it was stated above, the Reynold number, Re, is depend on the dimensionless axial velocity w (Equation (27)). From the definition of the magnetic number also, it is obtained that for a specific problem, (h, $\bar{\nu}$, $\bar{\rho} = \text{const}$) increasing Mn is equal with increasing the magnetic field strength. The increment of the magnetic field strength results to the rising of the force due to the magnetization at the transverse plane and as a consequence the secondary flow is generated, and strengthens as the magnetic field (Mn) strengthens. Thus, part of the kinetic energy towards the axial direction is converted, by the effect of the magnetic field, to kinetic energy at the transverse plane. Also, due to the way the magnetic field is applied there is no force due to the magnetic field towards the axial direction. Summarizing, increasing Mn strengthens the secondary flow, the axial velocity component reduces and finally the Re number decreases.

Another important flow characteristic, especially in BFD, is the skin friction coefficient at the walls. For its calculation the evaluation of the shear stresses is essential. Let $ABCD$ the plane where the flow is studied and $A'B'C'D'$ another plane, located one unit downstream and parallel to the previous one (see Figure 4).

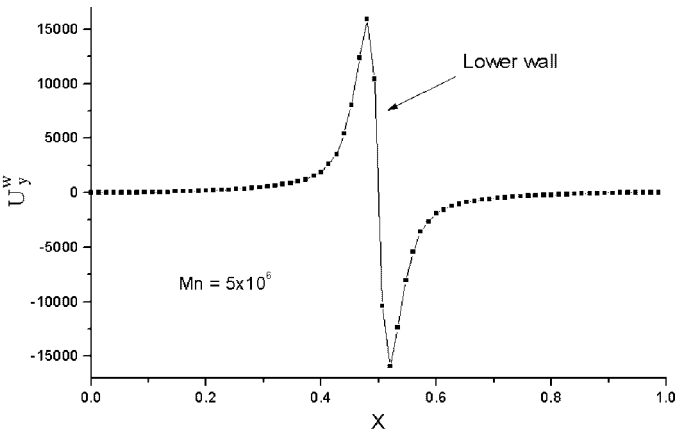

Figure 5. Variation of U_y^w on the lower wall with distance x.

The shear stresses acting at the $ABB'A'$ plane (lower wall) are the τ_{yx} and τ_{yz} in x and z directions, respectively, and are given by the relations

$$\tau_{yx} = \bar{\mu}\left(\frac{\partial \bar{u}}{\partial \bar{y}} + \frac{\partial \bar{v}}{\partial \bar{x}}\right)\Big|_{\bar{y}=0} = \bar{\mu}\,\frac{\partial \bar{u}}{\partial \bar{y}}\Big|_{\bar{y}=0} \overset{(8)}{=} \frac{\bar{\mu}\bar{v}}{h^2}\,\frac{\partial u}{\partial y}\Big|_{y=0} \tag{29}$$

and

$$\tau_{yz} = \bar{\mu}\left(\frac{\partial \bar{w}}{\partial \bar{y}} + \frac{\partial \bar{v}}{\partial \bar{z}}\right)\Big|_{\bar{y}=0} = \bar{\mu}\,\frac{\partial \bar{w}}{\partial \bar{y}}\Big|_{\bar{y}=0} \overset{(8)}{=} \frac{\bar{\mu}\bar{v}}{h^2}\,\frac{\partial w}{\partial y}\Big|_{y=0} \tag{30}$$

At the $AA'D'D$ plane (left wall) the acting stresses τ_{xy} and τ_{xz} are given by

$$\tau_{xy} = \bar{\mu}\left(\frac{\partial \bar{u}}{\partial \bar{y}} + \frac{\partial \bar{v}}{\partial \bar{x}}\right)\Big|_{\bar{x}=0} = \bar{\mu}\,\frac{\partial \bar{v}}{\partial \bar{x}}\Big|_{\bar{x}=0} \overset{(8)}{=} \frac{\bar{\mu}\bar{v}}{h^2}\,\frac{\partial v}{\partial x}\Big|_{x=0} \tag{31}$$

and

$$\tau_{xz} = \bar{\mu}\left(\frac{\partial \bar{u}}{\partial \bar{z}} + \frac{\partial \bar{w}}{\partial \bar{x}}\right)\Big|_{\bar{x}=0} = \bar{\mu}\,\frac{\partial \bar{w}}{\partial \bar{x}}\Big|_{\bar{x}=0} \overset{(8)}{=} \frac{\bar{\mu}\bar{v}}{h^2}\,\frac{\partial w}{\partial x}\Big|_{x=0} \tag{32}$$

respectively.

Thus, in order to calculate the stresses acting on the planes it is equivalent to calculate the non-dimensional quantities $\partial u/\partial y|_{y=0,1} = U_y^w$, $\partial v/\partial x|_{x=0,1} = V_x^w$, $\partial w/\partial y|_{y=0,1} = W_y^w$ and $\partial w/\partial x|_{x=0,1} = W_x^w$.

Figure 5 shows the variation of U_y^w with the dimensionless distance x, for the lower wall (plane $ABB'A'$, $y=0$), and for $\mathrm{Mn} = 5 \times 10^6$. It is observed that as x increases, U_y^w increases taking its maximum positive value near to the place were the wire is located ($x = 0.48$). For $x = 0.5$, U_y^w is equal to zero and afterwards decreases taking its minimum negative value for $x = 0.52$. As x further increases tending to $x = 1$, U_y^w is also increased taking, asymptotically, its limiting value zero. It is also remarked that the variation of $U_y^w(x)$, for the lower wall, is symmetrical with respect to the point $x = 0.5$, $U_y^w = 0$.

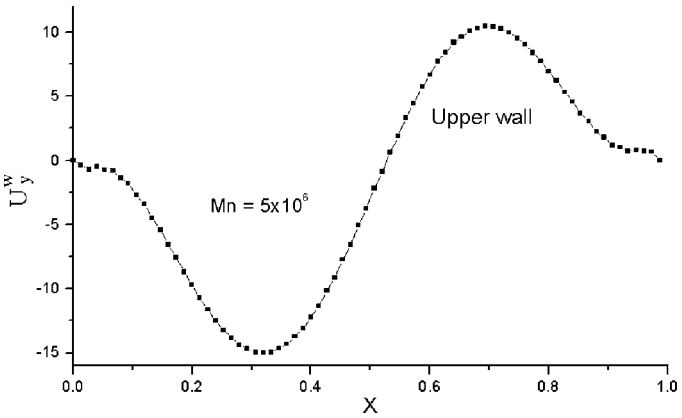

Figure 6. Variation of U_y^w on the upper wall with distance x.

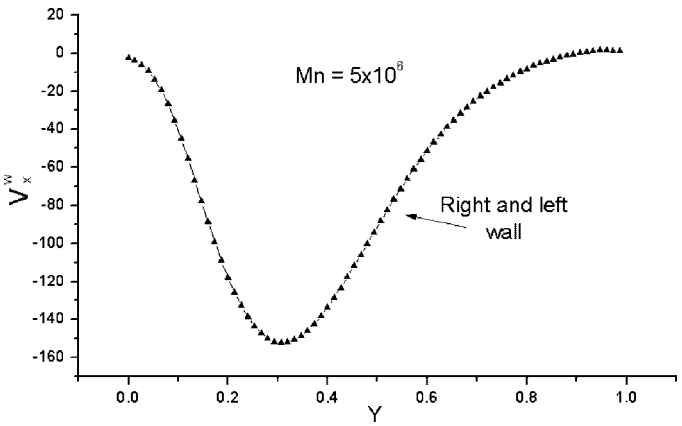

Figure 7. Variation of V_x^w on the left and right walls with distance y.

The variation of U_y^w, for the upper wall (plane $DCC'D'$, $y=1$) is presented in Figure 6. The behaviour of U_y^w is reversed with respect to that of the lower plane. However, in this case the variation is smooth having a parabolic character at each side of $x=0.5$ and a magnitude of three orders less than the corresponding one of the lower plane. This was expected since the magnetic field strength decreases as the distance y increases from the wire location.

Figure 7 shows the variation of V_x^w, with respect to y, for the right ($x=1$) and left wall ($x=0$). Owing to the symmetry of the flow field V_x^w varies in the same way for the right and left wall, it is negative for all y and its minimum value occurs at $y \approx 0.3$.

It is reminded that the velocities u, v and w are functions of the spatial co-ordinates x and y. As a consequence, the above-mentioned quantities, W_y^w and W_x^w are functions only of x and y, respectively. The variations of W^w, ($W^w = W_x^w$ or W_y^w) for all the planes with y or x, respectively, are shown in Figure 8. It is observed that W^w varies almost identically

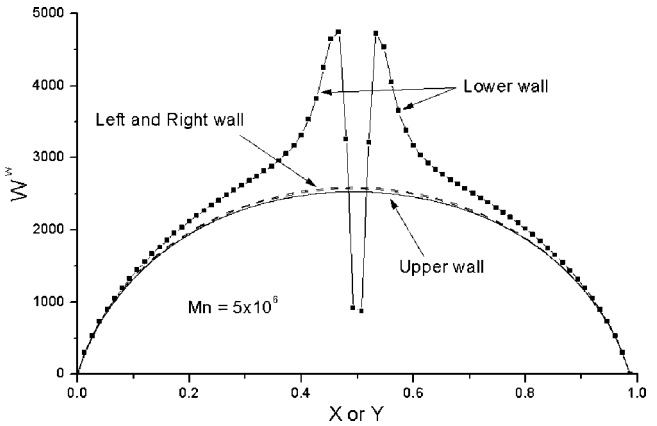

Figure 8. Variation of W^w on all walls with the corresponding distance x or y.

for all the planes except the lower one. For the lower wall it is observed an increase of W^w (W^w_y) moving towards the point $x = 0.5$. However, close to $x = 0.5$ and within the interval $[0.46, 0.54]$ a rapid decrement in the values of W^w takes place and the minimum value occurs exactly on $x = 0.5$.

The obtained numerical results are similar to those obtained from Bashtovoy *et al.* for non-conducting magnetic fluid (FHD). For the fully developed flow in a straight rectangular duct, under the action of an applied magnetic field, they observed that two vortices where risen at the transverse plane, whereas the axial velocity reduced [16].

It is apparent that the application of the magnetic field affects considerably the flow field as well as the shear stresses, especially close to the area of the magnetic pole. These conclusions suggest that a careful choice of the imposed magnetic field will affect the flow characteristics and hence can be utilized for possible medical and engineering applications.

6. EXISTENCE AND UNIQUENESS OF SOLUTIONS

As already mentioned, the well-known ADI method was used for the calculation of u^*, v^* and w^*. For the demonstration of the existence and uniqueness of the above-mentioned solutions of Equations (10)–(12), we will use Equation (16) with the asterisks omitted.

$$\frac{\partial u}{\partial t} + u\frac{\partial u}{\partial x} + v\frac{\partial u}{\partial y} = -\frac{\partial p}{\partial x} + \frac{\partial^2 u}{\partial x^2} + \frac{\partial^2 u}{\partial y^2} + \mathrm{Mn}\, H\frac{\partial H}{\partial x} \tag{33}$$

During the first half of the ADI method (y-constant) an equation is obtained of the form

$$\begin{aligned} &C_1(u, \Delta x)u(i-1, j) + C_2(\Delta x, \Delta t)u(i, j) + C_3(u, \Delta x)u(i+1, j) \\ &\quad = Rhs(u, v, p, \Delta x, \Delta t, Mn), \quad i = 1, \ldots, M, \ j = 1, \ldots, N \end{aligned} \tag{34}$$

In order to study the existence and the uniqueness of the solution of this equation we consider that the non-linear terms are at the same time level.

Equation (34) is a non-linear difference equation with respect to u and can be transformed, by setting $i = i + 1$ and after some manipulation, to the non-linear partial difference equation.

$$u(i+2,j) + u(i,j) - \frac{2(\Delta t + \Delta x^2)}{\mathrm{d}t}\, u(i+1,j) = G(i,j) - \frac{\Delta x}{2}\, u(i+1,j)u(i,j) + \frac{\Delta x}{2}\, u(i+1,j)u(i+2,j) \tag{35}$$

where

$$G(i,j) = \Delta x^2(-H(i,j)H_x(i,j) + P_x(i,j) - u_{yy}(i,j) + u_y(i,j)v(i,j)) - \frac{2\Delta x^2 u(i,j)}{\Delta t}$$

and the subscripts denote partial differentiation, e.g. $(\ )_x = \partial(\ )/\partial x$, $(\ )_y = \partial(\ )/\partial y$.

Equation (35) has a unique solution in the Banach space $l^1_{\mathbb{N}_M \times \mathbb{N}_N}$ of all complex sequences that are summable, i.e. in the space

$$l^1_{\mathbb{N}_M \times \mathbb{N}_N} = \left\{ u(i,j) : \mathbb{N}_M \times \mathbb{N}_N \to \mathbb{C} \;\middle/\; \sum_{i=1}^{M} \sum_{j=1}^{N} |u(i,j)| < +\infty \right\} \tag{36}$$

where $\mathbb{N}_M = \{1,\ldots,M\}$, $\mathbb{N}_N = \{1,\ldots,N\}$, provided that *one* of the following three criteria is satisfied [17, Theorem 3.1, relations (3.13), (3.14), (3.13), respectively].

Criterion 1:

$$\sum_{j=1}^{N} |u(1,j)| + \sum_{j=1}^{N} |u(2,j)| + \sum_{i=1}^{M-1} \sum_{j=2}^{N} |G(i,j)| - \frac{\Delta x}{4(3\Delta t + \Delta x \Delta t + 2\Delta x^2)} < 0 \tag{37}$$

Criterion 2:

$$\sum_{i=1}^{M-1} \sum_{j=2}^{N} |G(i,j)| - \frac{\Delta x}{4(3\Delta t + \Delta x \Delta t + 2\Delta x^2)} < 0 \tag{38}$$

Criterion 3:

$$\sum_{j=1}^{N} |u(1,j)| + \frac{\Delta t}{2(\Delta t + \Delta x^2)} \sum_{i=1}^{M-1} \sum_{j=2}^{N} |G(i,j)| - \frac{\Delta t + \Delta x^2}{2\Delta t(2 + \Delta x)} < 0 \tag{39}$$

We mention here that the other conditions required in Reference [17, Theorem 3.1] are automatically satisfied.

On the contrary, the second half of the ADI method gives the following linear difference equation with respect to the unknown variable u

$$C_1(v,\Delta y)u(i,j-1) + C_2(\Delta y,\Delta t)u(i,j) + C_3(v,\Delta y)u(i,j+1) = \mathrm{Rhs}(u,p,\Delta y,\Delta t,Mn), \quad i = 1,\ldots,M,\ j = 1,\ldots,N \tag{40}$$

Equation (40) can be transformed, after some manipulation, to the following linear partial difference equation:

$$u(i,j+1)=\frac{-2}{-2+\Delta y v(i,j)}\,G(i,j)+a_1(i,j)u(i,j-1)+b_1(i,j)u(i,j)$$

where

$$a_1(i,j)=\frac{2+\Delta y v(i,j)}{-2+\Delta y v(i,j)},\quad b_1(i,j)=\frac{-4(\Delta t+\Delta y^2)}{\Delta t(-2+\Delta y v(i,j))}$$

For this case, the existence and the uniqueness of the solution of (40) is ensured in the Hilbert space $l^2_{\mathbb{N}_M\times\mathbb{N}_N}$ of all complex sequences that are square summable, i.e. in the space

$$l^2_{\mathbb{N}_M\times\mathbb{N}_N}=\left\{u(i,j):\mathbb{N}_M\times\mathbb{N}_N\to\mathbb{C}\;\middle/\;\sum_{i=1}^{M}\sum_{j=1}^{N}|u(i,j)|^2<+\infty\right\} \tag{41}$$

provided that one of the following three criteria is satisfied [18, Theorem 3.1, relations (3.2), (3.4), (3.3), respectively].

Criterion 1:

$$\sup|a_1|+\sup|b_1|-1<0 \tag{42}$$

Criterion 2:

$$\sup\left|\frac{1}{b_1}\right|<+\infty\quad\text{and}\quad\sup\left|\frac{1}{b_1}\right|(1+\sup|a_1|)-1<0 \tag{43}$$

Criterion 3:

$$\sup\left|\frac{1}{a_1}\right|<+\infty\quad\text{and}\quad\sup\left|\frac{1}{a_1}\right|(1+\sup|b_1|)-1<0 \tag{44}$$

We mention here that the other conditions required in Reference [18, Theorem 3.1] are automatically satisfied.

It is worth mentioning here that the spaces defined by (36) and (41) are suitable for studying partial difference equations, arising by the application not only of ADI method but also of other numerical methods, in the study of physical problems. The theoretical results of References [17, 18] concern the existence and the uniqueness of non-linear and linear partial difference equations in the more general spaces $l^1_{\mathbb{N}\times\mathbb{N}}$ and $l^2_{\mathbb{N}\times\mathbb{N}}$, which are defined as in (36) and (41), but now the indexes of the appearing sums are from $1\sim\infty$. In order to use these results we had considered zero infinite elements outside the computational domain.

Also, these theoretical results concern complex sequences which, of course, include the real sequences that we use. We should point out here that the criteria given above are sufficient but not necessary for the existence and the uniqueness of the solutions of the difference equations under consideration. Thus, if no one of the three criteria, mentioned above, is satisfied we cannot conclude anything (at least with this method) about the existence and the uniqueness of the solutions of the corresponding equations. Similar criteria hold also for the linear and non-linear partial difference equations that describe the first and second step of the ADI method for the partial differential equations corresponding to v and w.

Table III. Calculated values of the right-hand sides of criteria of existence and uniqueness for various equations and magnetic numbers.

Equation	Criterion 1	Criterion 2	Criterion 3	Mn
First half of ADI for U	-0.044×10^{0}	0.172×10^{-2}	-0.173×10^{0}	0.0
Second half of ADI for U	0.140×10^{2}	-0.857×10^{0}	0.140×10^{2}	0.0
First half of ADI for V	0.140×10^{2}	-0.857×10^{0}	0.140×10^{2}	0.0
Second half of ADI for V	-0.225×10^{3}	0.172×10^{-2}	-0.173×10^{0}	0.0
First half of ADI for W	0.140×10^{2}	0.140×10^{2}	-0.857×10^{0}	0.0
Second half of ADI for W	0.140×10^{2}	-0.857×10^{0}	0.140×10^{2}	0.0
First half of ADI for U	0.196×10^{4}	0.236×10^{5}	0.168×10^{4}	0.1×10^{7}
Second half of ADI for U	0.220×10^{2}	-0.763×10^{0}	0.261×10^{2}	0.1×10^{7}
First half of ADI for V	0.164×10^{2}	-0.813×10^{0}	0.213×10^{2}	0.1×10^{7}
Second half of ADI for V	0.174×10^{4}	0.236×10^{5}	0.168×10^{4}	0.1×10^{7}
First half of ADI for W	0.164×10^{2}	0.213×10^{2}	-0.813×10^{0}	0.1×10^{7}
Second half of ADI for W	0.220×10^{2}	-0.763×10^{0}	0.261×10^{2}	0.1×10^{7}
First half of ADI for U	0.471×10^{4}	0.565×10^{5}	0.403×10^{4}	0.2×10^{7}
Second half of ADI for U	0.435×10^{2}	-0.509×10^{0}	0.611×10^{2}	0.2×10^{7}
First half of ADI for V	0.200×10^{2}	-0.749×10^{0}	0.344×10^{2}	0.2×10^{7}
Second half of ADI for V	0.448×10^{4}	0.565×10^{5}	0.403×10^{4}	0.2×10^{7}
First half of ADI for W	0.200×10^{2}	0.344×10^{2}	-0.749×10^{0}	0.2×10^{7}
Second half of ADI for W	0.435×10^{2}	-0.509×10^{0}	0.611×10^{2}	0.2×10^{7}
First half of ADI for U	0.866×10^{4}	0.104×10^{6}	0.742×10^{4}	0.3×10^{7}
Second half of ADI for U	0.272×10^{3}	0.219×10^{0}	0.451×10^{3}	0.3×10^{7}
First half of ADI for V	0.254×10^{2}	-0.652×10^{0}	0.599×10^{2}	0.3×10^{7}
Second half of ADI for V	0.843×10^{4}	0.104×10^{6}	0.742×10^{4}	0.3×10^{7}
First half of ADI for W	0.254×10^{2}	0.599×10^{2}	-0.652×10^{0}	0.3×10^{7}
Second half of ADI for W	0.272×10^{3}	0.219×10^{0}	0.451×10^{3}	0.3×10^{7}
First half of ADI for U	0.144×10^{5}	0.172×10^{6}	0.123×10^{5}	0.4×10^{7}
Second half of ADI for U	0.489×10^{3}	0.531×10^{0}	0.997×10^{3}	0.4×10^{7}
First half of ADI for V	0.343×10^{2}	-0.493×10^{0}	0.115×10^{3}	0.4×10^{7}
Second half of ADI for V	0.141×10^{5}	0.172×10^{6}	0.123×10^{5}	0.4×10^{7}
First half of ADI for W	0.343×10^{2}	0.115×10^{3}	-0.493×10^{0}	0.4×10^{7}
Second half of ADI for W	0.489×10^{3}	0.531×10^{0}	0.997×10^{3}	0.4×10^{7}
First half of ADI for U	0.222×10^{5}	0.267×10^{6}	0.190×10^{5}	0.5×10^{7}
Second half of ADI for U	0.917×10^{4}	0.121×10^{3}	0.233×10^{5}	0.5×10^{7}
First half of ADI for V	0.504×10^{2}	-0.205×10^{0}	0.261×10^{3}	0.5×10^{7}
Second half of ADI for V	0.220×10^{5}	0.267×10^{6}	0.190×10^{5}	0.5×10^{7}
First half of ADI for W	0.504×10^{2}	0.261×10^{3}	-0.205×10^{0}	0.5×10^{7}
Second half of ADI for W	0.917×10^{4}	0.121×10^{3}	0.233×10^{5}	0.5×10^{7}

In order to verify which of the above-mentioned criteria is satisfied we compute the left-hand sides of criteria (37)–(39) or (42)–(44), numerically, and we examine if the quantity on the left-hand side of these criteria is negative. Table III shows the computed values of the quantity on the left-hand side of each criterion. It is reminded that the criteria are different for each step of the ADI method and for each one of the equations with respect to u, v and w. Notice that for $\mathrm{Mn} = 0$, at least one of the criteria is satisfied and the existence and the uniqueness of the solutions for the two steps of ADI method, for all equations is ensured. For $\mathrm{Mn} = 1 \times 10^6$–$2 \times 10^6$ no one of the criteria is satisfied for the first and second half of ADI method for u and v momentum equation, respectively. Finally, for $\mathrm{Mn} = 3 \times 10^6$–$5 \times 10^6$ at least one of the criteria is satisfied only for the first half of v and w momentum equations, respectively. Consequently, we can strictly assure the existence and the uniqueness of the solutions *only* in some steps of the ADI method for u, v and w.

7. CONCLUDING REMARKS

In this work the three-dimensional, fully developed, viscous flow of a biomagnetic fluid in a rectangular channel in the presence of an applied magnetic field is studied. Numerical results, by using an efficient technique based on a pressure-linked pseudotransient method applied on a common orthogonal grid are obtained. The increment of the magnetic field strength leads to the formation of two vortices as far as concerns the secondary flow, whereas the axial flow is retarded. This phenomenon is extended, especially close to the source of the magnetic field, as the magnetic field strength increases. The shear stresses acting on the walls of the channel are also calculated. It was found that the magnetic field considerably influence these stresses, especially those acting on the lower plane near of which is the source of the magnetic field. Criteria are given concerning the existence and the uniqueness of the solution of the linear and non-linear partial difference equations, resulting after the discretization of the momentum equations applying the ADI method. The existence and the uniqueness of solution, obtained by the ADI method, is ensured only for some of the difference equations, whereas for the remaining, at least with the theory that was used, there is no answer.

ACKNOWLEDGEMENTS

The authors are grateful to Dr Eugenia N. Petropoulou, Department of Engineering Science, for making comments and suggestions for improving their article.

REFERENCES

1. Haik Y, Pai V, Chen CJ. Development of magnetic device for cell separation. *Journal of Magnetism and Magnetic Materials* 1999; **194**:254–261.
2. Ruuge EK, Rusetski AN. Magnetic fluid as drug carriers: targeted transport of drugs by a magnetic field. *Journal of Magnetism and Magnetic Materials* 1993; **122**:335–339.
3. Plavins J, Lauva M. Study of colloidal magnetite binding erythrocytes: prospects for cell separation. *Journal of Magnetism and Magnetic Materials* 1993; **122**:349–353.
4. Higashi T, Yamagishi A, Takeuchi T, Kawaguchi N, Sagawa S, Onishi S, Date M. Orientation of erythrocytes in a strong static magnetic field. *Journal of Blood* 1993; **82**(4):1328–1334.
5. Takeuchi T, Mizuno T, Higashi T, Yamagishi A, Date M. Orientation of red blood cells in high magnetic field. *Journal of Magnetism and Magnetic Materials* 1995; **140–144**:1462–1463.

6. Higashi T, Ashida N, Takeuchi T. Orientation of red blood cells in static magnetic field. *Physica B* 1997; **237–238**:616–620.
7. Pauling L, Coryell CD. The magnetic properties and structure of hemoglobin, oxyhemoglobin and carbonmonoxy hemoglobin. In *Proceedings of the National Academy of Science*, vol. 22, USA, 1936; 210–216.
8. Haik Y, Chen JC, Pai VM. Development of bio-magnetic fluid dynamics. In *Proceedings of the IX International Symposium on Transport Properties in Thermal Fluids Engineering*, *Singapore*, *Pacific Center of Thermal Fluid Engineering*, Winoto SH, Chew YT, Wijeysundera NE (eds), vol. 25–28, Hawaii, USA, June 1996; 121–126.
9. Matsuki H, Yamasawa K, Murakami K. Experimental Considerations on a new automatic cooling device using temperature sensitive magnetic fluid. *IEEE Transactions on Magnetics* 1977; **Mag-13**(5):1143–1145.
10. Fertman VE. *Magnetic Fluids Guidebook*: *Properties and Applications*. Hemisphere: New York, 1990.
11. Rosensweig RE. *Ferrohydrodynamics*. Dover: Mineola, NY, 1985.
12. Fletcher CAJ. *Computational Techniques for Fluid Dynamics 1* (2nd edn). Springer: Berlin, 1991.
13. Patankar SV. *Numerical Heat transfer and Fluid Flow*. Hemisphere: Washington, DC, 1980.
14. Hatzikonstantinou P. Unsteady mixed convection about a porous rotating sphere. *International Journal of Heat and Mass Transfer* 1990; **33**(1):19–27.
15. Pedley TL. *The Fluid Mechanics of Large Blood Vessels*. Cambridge University Press: Cambridge, MA, 1980.
16. Bashtovoy VG, Berkovsky BM, Vislovich AN. *Introduction to Thermomechanics of Magnetic Fluids*. Hemisphere: Washington, DC, Springer: Berlin, 1988.
17. Petropoulou EN, Siafarikas PD. Solutions of non-linear delay and advanced partial difference equations in the space $l^1_{\mathbb{N}\times\mathbb{N}}$. *Computer and Mathematics with Application* (Special issue: Advanced in Difference equations IV) 2003; **45**:905–934.
18. Petropoulou EN, Siafarikas PD. Bounded solutions of a class of linear delay and advanced partial difference equation. *Dynamical System and Applications* 2001; **10**:243–260.

